+ MODEL

Available online at www.sciencedirect.com

ScienceDirect

Solid Earth Sciences 9 (2024) 100187

www.elsevier.com/locate/SESCI

Origin of continental red beds: Warming from above or heating from below?

Lianting Jiang [a], Chun'an Tang [b,c,d,*], Bin Gong [e,**], Zhen Chen [f], Tiantian Chen [g], Zhanjie Qin [h], Guoneng Chen [f]

[a] *Key Laboratory of Ocean and Marginal Sea Geology, South China Sea Institute of Oceanology, Chinese Academy of Sciences, Guangzhou 510301, China*
[b] *State Key Laboratory of Coastal & Offshore Engineering, Dalian University of Technology, Dalian 116024, China*
[c] *Computational Geoscience Research Center, Chengdu University of Technology, Chengdu 610059, China*
[d] *State Key Laboratory of Geological Processes and Mineral Resources, China University of Geosciences (Wuhan), Wuhan 430074, China*
[e] *Department of Civil and Environmental Engineering, Brunel University London, London UB8 3PH, UK*
[f] *School of Earth Sciences and Geological Engineering, Sun Yat-sen University, Guangzhou 510275, China*
[g] *School of Resources and Civil Engineering, Northeastern University, Shenyang 110819, China*
[h] *Key Laboratory of Comprehensive and Highly Efficient Utilization of Salt Lake Resources, Qinghai Institute of Salt Lakes, Chinese Academy of Sciences, Xining 810008, China*

Received 19 December 2023; revised 14 May 2024; accepted 22 May 2024
Available online ■ ■ ■

Abstract

The formation of continental red beds is generally considered to be related to an arid climate. Heating experiments (performed by L.J. and G.C.) using dried black mud sediment also demonstrate that the reddening may be caused by the transformation of goethite to haematite that begins at approximately 150 °C under anhydrous conditions, and increasing the temperature to 450 °C is positively correlated with the red colour and peak value of haematite. If this process applies to continental red beds, it implies a thermal origin of red beds as a result of high diagenetic temperatures rather than as the cause of their deposition under an arid climate. Namely, subsiding red-bed basins are heated from below rather than warmed from above. Here, we further strengthen this idea by new evidence from borehole cores drilled from red beds in SE China, showing a clear geological section from the surface soil to red beds to bottom granite. The data reveal that the continental red beds formed at least at a temperature within 150–400 °C, and the underlying granite usually formed at temperatures greater than 600 °C. Our results imply a possible relationship between continental red bed events and Earth's thermal cycles.

Keywords: Red bed; Formation mechanism; Haematite; High diagenetic temperature; Arid climate

1. Introduction

Although significant advances towards understanding the onset of continental red beds have been made in the last decade, the generation mechanism of continental red beds remains controversial. Schmalz (1968) suggested that their formation can be recognized as the result of arid climate. Meanwhile, the paleolatitudes and paleocontinents can be reconstructed by their distribution (Seyfert and Sirkin, 1979). Walker (1967) investigated the sediments at the Sonoran Desert in the United States and adjacent Mexico and discussed the formation of several red beds because of the hot and dry climate. Most of the previous studies in SE China also believed that the continental red beds occurred under hot/arid climate conditions (Li et al., 2009).

However, although favoured by desert condition, in situ pigmentation can also form within sediments consisting of unstable iron-bearing minerals under less dry climates. Several

* Corresponding author.
** Corresponding author.
E-mail addresses: tca@mail.neu.edu.cn (C. Tang), bin.gong@brunel.ac.uk (B. Gong).
Peer review under responsibility of Guangzhou Institute of Geochemistry.

https://doi.org/10.1016/j.sesci.2024.100187

studies indicate that an arid climate is not necessary for the occurrence of red beds because the existence of haematite is generally automorphic (Van Houten, 1973; Turner, 1980). For example, the Pleistocene red beds in Tanzania formed under hundred millimetres of rainfall per year (Van Houten, 1973). The fluvial red-bed deposits in early Cenozoic in Utah (Picard, 1971) and the pigmented sandstones in the Jurassic Morrison Formation on the Colorado Plateau (Bowers and Shawe, 1961) formed in savanna environment (Van Houten, 1973). Preserved remains of plants and animals are extremely rare in red beds. However, molecular fossils have been found in Middle Jurassic–Early Cretaceous red beds at Jianmenguan in the Sichuan Basin, China. This finding indicates the abundance of woody rather than grassy vegetation and implies a warm and humid climate. Besides, the paleobiology and petrology of the rare and massive siliceous woods preserved in the Guantou Formation of the Early Cretaceous red bed basin in Xinchang County, China show that the paleoclimate during this time was basically warm and moist (Xue et al., 2005). Additionally, because of the dinosaur eggs found in many red-bed basins in SE China (Wang et al., 2012) the questions of whether the climate had arid or desert conditions during red bed formation and how such large animals could survive also arise. These findings cast doubt on the correlation between red-bed formation and arid climate during deposition, and the significance of red beds in paleoclimatology remains unclear (Chukhrov, 1973).

A significant challenge to the suggestion of an arid climate causing the red bed formation is the worldwide distribution of marine red beds in deep ocean environments. These oceanic red beds are present throughout geological history, particularly since the beginning of the Phanerozoic, especially in oceanic bottom and pelagic settings (Song et al., 2017). Although it is recognised that, in continental environment, the red colour predominantly results from the existence of haematite (Cai et al., 2012), the occurrence of the haematite pigment in red beds has aroused controversy. Due to the lack of a documented modern analogue, the detailed development of the red pigment mechanism in red bed deposits is complex and difficult to decipher (Van Houten, 1973). There are two main conflicting presumptions on the origin of haematite (Walker, 1967). One hypothesis regards the haematite as an allochthonous mineral that was transported to the sites of sedimentation mixed with clays from the weathering areas of the humid tropics. This hypothesis contends that the haematite occurs in lateritic soils at wet tropical/subtropical sources, and then is transported to desert basins where it can be preserved. Eventually, it becomes connected with evaporites forming in the basins (Walker, 1967); however, the opposing hypothesis supports an authigenic view that the haematite forms only after deposition because of in situ alteration of iron-bearing detrital grains under hot, semiarid or arid climates (Walker, 1967) as the result of goethite dehydration (Chukhrov, 1973). Since both hypotheses require an arid climate, they do not apply to marine red beds.

The key factor that has not been satisfactorily explained is the environment in which the haematite can form via the goethite dehydration, which is in a finely divided and poorly crystallised process and contributes to the majority of the pigmenting material. We suggest that the haematite pigments in continental red bed deposits are predominantly of diagenetic origin, and such pigments in the sediments can reflect the special conditions of crustal alteration subject to a higher temperature after deposition rather than the certain weathering conditions at the source areas. According to Chen and Grapes (2007), Weibel and Grobety (1999), Turner (1980), Walker (1976) and van Houten (1973), the dyestuff within the continental red beds primarily originates from fine authigenic hematite, while goethite and ferrihydrite are predominantly contained inner younger sediments. An illustrative instance of the goethite-to-hematite transition with increasing depth (and temperature) is showcased in the Skagerrak Formation, Denmark, as outlined by Weibel and Grobety (1999). At shallower depths, up to 550 m, goethite is the sole Fe-oxide present, whereas at deeper levels, hematite gradually emerges and becomes more prevalent relative to goethite. Remarkably, hematite crystals in the deeper layers of the Skagerrak Formation retain the same morphology and size as goethite crystals in shallower levels, owing to pseudomorphic replacement. Simultaneously, goethite can be treated as the precursor to hematite in red bed formation. Experimental findings by Dekkers (1990) and DeBoer and Dekkers (2001) have pinpointed the temperature range for goethite transformation to hematite to be approximately between 150 and 400 °C. The corresponding observations and test data collectively suggest: (1) The formation of red pigment in rocks necessitates a diagenetic temperature of no less than 150 °C; (2) Red beds generated within a tectono–sedimentary cycle exhibit a striking contrast: they display shades of gule or maroon in their lower and middle sections, while transitioning to gray-black hues in the uppermost part (see Fig. 1a). This color variation hints at distinct diagenetic conditions; notably, the upper gray-black segment suggests diagenetic temperatures below 150 °C. This observation offers valuable insights, proposing an estimated location for the 150 °C paleo-isotherm precisely at the transition from red to gray-black layers.

On the above studies, a geological model concerning the thermal cause of the Meso-Cenozoic red beds in SE China has been set up by Chen and Grapes (2007) in studies of granite formation (Fig. 1b). The hypothesis suggests that crustal (lithospheric) temperature increases can trigger the melting of continental crust into granitic magma and even influence basinal sediment diagenesis. High geothermal temperatures in the bottom of the basins can accelerate deep-level downwards percolation of oxygen-rich surface water, rapidly heat this water, and vapourize the water upwards to form gas−liquid fluid circulation, which drives material migration and evolution in the sedimentary system. When the temperatures of basinal bottom sediments reach ~150 °C, goethite starts to dehydrate to haematite, giving the red colour to sediments, and the high-temperature and oxidising environment decomposes the organic matter and sulphides in the red beds. Meanwhile, the fluids continuously extract metals (*e.g.*, Cu, Pb–Zn) from the red beds. With the consumption of free oxygen and the

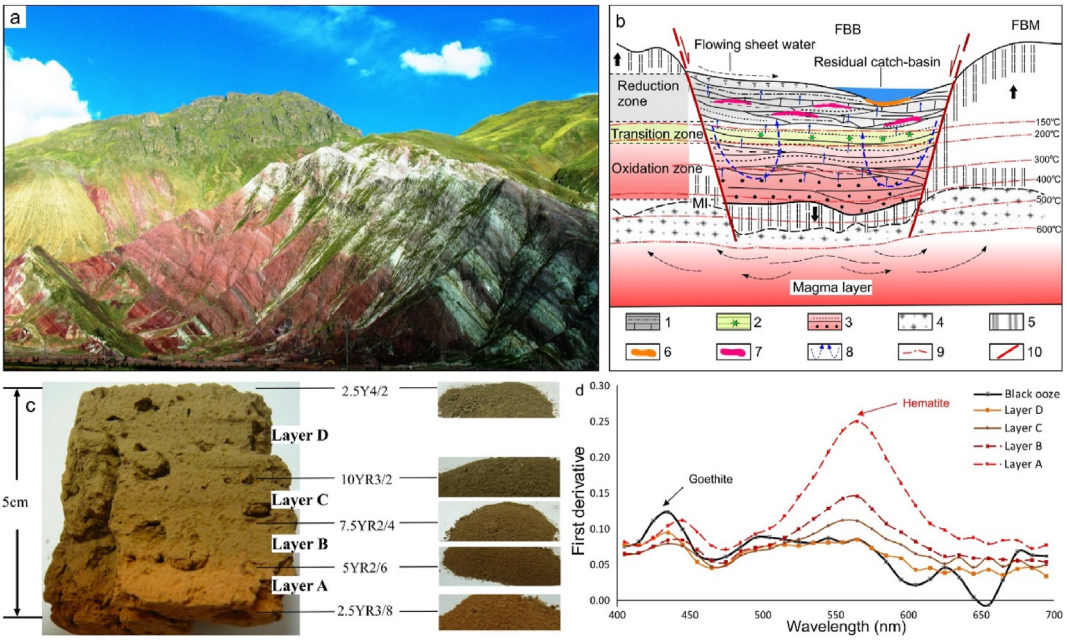

Fig. 1. a. Vertical colour zonation of a tilted red-bed sequence with comparison to the thermal origin of continental red beds (after Chen and Grapes (2007); b. Modelling of the thermal origin of continental red beds indicating the correlation between diagenetic temperature and colour variation in the sedimentary sequence (after Chen and Grapes (2007): 1 grey−black (reduced) zone, mainly mudstone and carbonates with saline and oil–gas deposits, 2 yellow−green (transitional redox) zone, mainly sandstone with Cu mineralization, 3 red (oxidation) zone, mainly conglomerate and sandstone, 4 granite, the semisolidified upper part of the crustal magma layer, 5 basement rock, 6 halite, 7 oil–gas deposit, 8 direction of fluid movement during diagenesis, 9 inferred isotherms with temperatures, 10 fault; c. unilateral heating experiment on modern sediments simulating geothermal process on sediment diagenesis. The temperatures of the sample bottom and top are ~300 °C and ~70 °C, respectively. The colour pattern (black above red) appeared after seven days of heating (after Jiang et al. (2015)); d. DRS first derivative curves of 4 mud subsamples of the heated samples in Fig. 1c (after Jiang et al. (2015)).

concentration of large amounts of base/alkali metal ions, the fluid pH values gradually increase, and its Eh values gradually decrease, and these fluids are driven upwards in the sedimentary system by the temperature−pressure gradient. During their ascent, the ore-forming materials in the gas−liquid fluids precipitate due to the temperature−pressure drop and pH–Eh variation, forming oil and gas, halite and Cu–Pb–Zn sulphide deposits (Fig. 1a and b). This model can well explain the origin of red bed pigments, as well as the formation of a complete red bed system, *i.e.*, (from bottom up) red beds with high oxygen fugacity, greyish yellow–greyish green beds near redox interfaces where sulphides commonly develop, and black beds in reducing environments where oil–gas and halite deposits commonly develop. Additionally, the continental red bed forms through the dynamic interplay of thermal energy exchange between the sedimentary basin and the deep crustal heat source as a consequence of the inner thermal conduction of the Earth.

2. Methodology

To test the model, the first and last authors carried out experiments in which the black mud was gradually heated to simulate the red-bed formation (Jiang et al., (2015)). After naturally air-drying, the light brown mud block, measuring 10 cm × 10 cm × 5 cm, underwent subdivision into four subsamples. Subsamples 1, 2, and 3 were individually pulverized to 200-mesh using an agate mortar. A portion of subsample 1 underwent examination through diffuse reflectance spectroscopy (DRS), while the rest was subjected to immersion in a 5% acetic acid and 10% hydrogen peroxide solution. Post-rinsing with distilled water, the components were separated via centrifuge and subsequently dried at 55 °C for X-ray diffraction analysis. Subsamples 2 and 3 were heated separately in Experiments 1 and 2. Subsample 4 remained intact as a 5 cm × 5 cm × 5 cm block for Experiment 3. In Experiment 1, approximately 50g of subsample 2 powder underwent heating at a consistent 450 °C in a muffle furnace for durations of 1, 2, 5, 8, 12, 24, and 64 h. Following heating, seven samples were subjected to DRS analysis. Experiment 2 involved dividing subsample 3 powder (~50g) into seven equal portions, each subsequently heated for 24 h in a muffle furnace at temperatures ranging from 150 °C to 450 °C in an increment of 50 °C, then analysed using DRS. For Experiment 3, subsample 4 was heated on an electric hot plate at 450 °C for 7 days. Four samples were extracted at intervals of 0–1, 1–2, 2–3, and 3–5 cm from the base of the heated block, pulverized to 200-mesh, and analysed via DRS.

Furthermore, to analyse the content of iron oxides in sediments and their staining reactions, the Perkin–Elmer Lambda 950 was applied, by which the DRS analysis can be performed through an ultraviolet, visible and near-infrared spectrophotometer, and the first derivative curve of reflected light intensity in the visible light band (400–700 nm) can be obtained. Meanwhile, to discriminate the oxidation-reduction environment during the sedimentary diagenetic stage of samples, the PANalytical-PW2424 fluorescence spectrometer was used to

analyze the content of major elements in the samples. Simultaneously, the ferrous content can be determined by the acid digestion and potassium dichromate titration (Fe-VOL05) method, and the Fe^{3+}/Fe^{2+} ratio can be calculated. Additionally, the SIGMA-type field emission scanning electron microscopy was utilized to observe the mineral composition and microstructure characteristics of the samples.

The heating experiments demonstrated that the reddening process is induced by the alteration of goethite into haematite which starts at 150 °C under the anhydrous environment. Unilateral heating experiments on modern sediments in which the DRS shows the distinct goethite peak at 435 nm (Fig. 1d) simulate geothermal processes during sediment diagenesis. After sustaining the temperatures of the sample bottom and top at ~300 °C and ~70 °C, respectively, for 7 days, the sample displays a gradient colour stripe from red at the lower part to greyish yellow at the upper part, which is typically similar to a complete red bed sequence (Fig. 1c). The first derivative curves of four subsamples chosen from various vertical intervals (Fig. 1c) display that as the temperature from layer D (top) to layer A (base) of the sample increases, the goethite peaks at 435 nm continuously decrease until almost disappearing. Meanwhile, a clay mineral peak at 445 nm occurs, and the haematite peaks at 565 nm increase rapidly. The experimental results show that irons in black mud are predominantly as goethite, and increasing temperature (>150 °C, which is the initial dehydration temperature of goethite to haematite) is accompanied with the drop of goethite and the growth of haematite, consequently turning the samples red. The results strongly support the idea of a thermal onset for continental red beds.

If these experimental results apply to red beds, it implies red beds possibly originated from high geothermal temperature during diagenesis. Since the diagenetic temperatures obtained from experiments are approximately 150–400 °C (Jiang et al., 2015), if the experiment is reliable, it is clear that fine-grained goethite under virtually all thermal conditions is thermodynamically unstable and decomposed to haematite plus water, *i.e.* the goethite dehydration to haematite during sediments burial with increasing geothermal temperature. Hence, some ancient red beds might originally deposit without their red colour but turned to red later during high-temperature diagenesis (Chen and Grapes, 2007). If this formation process occurred, haematite can undoubtedly be used as an indicator of high-temperature environments.

Here, we further strengthen this conclusion by showing evidence from a site investigation with a borehole core drilled from red-bed basin in SE China. The proposed thermal model clarifies the vertical colour, temperature, redox and mineral zonation of red-bed sequence in SE China, from red (haematite-bearing) to green−yellow (Cu, Zn, and V sulphide mineralization) to grey−black (hydrocarbon and halite-bearing) sediments. Meanwhile, this model can foster the exploration of hydrocarbon & halite deposition at the red-bed basins in SE China (Chen and Grapes, 2007; Jiang et al., 2015). Recently, a borehole was drilled into Late Cretaceous strata located under the Quaternary system in the Pearl River Delta on the northern coast of the South China Sea. The strata are composed of mainly (silty-) mudstone and marl with little difference in lithology, exhibiting a complete vertical downwards colour sequence of red beds from grey dark, cinerous to maroon and red (Fig. 2a), and this sequence can be compared with the geological section, model and experimental result displayed in Fig. 1. The sediments were systemically sampled (Fig. 2a) and analysed, and their Fe^{3+}/Fe^{2+} ratios show a gradual increase with burial depth (Fig. 2b), indicating a reductive diagenetic environment for the grey dark and cinerous sediments (Fe^{3+}/Fe^{2+} ratios <1) in the upper borehole and an oxidising diagenetic environment for the underlying red bed (Fe^{3+}/Fe^{2+} ratios >1, among which the ratios of the maroon beds increase to 1–3 and those of the red beds increase to >3). The DRS 1st derivative curves of the grey dark and cinerous sediments show no obvious ferric oxide peaks, but the underlying red bed curves show 565 nm peaks as the outcome of haematite, which occur in the goethite pseudomorph (Fig. 3b and c), implying that they may have formed via goethite dehydration during sediment diagenesis. The haematite peak heights of the curves for the red beds gradually increase as burial depth increases (Fig. 3a); such variations (from shallow samples to deep samples) are similar to those in the simulation experiment from low temperatures (70 °C) to high temperatures (300 °C) (Figs. 1d and 2c), suggesting that the haematite pigments of red beds originated from high geothermal temperatures (>150 °C) and that the haematite content increases with burial depth. The formation of a red bed system in which the upper grey dark and cinerous sediments formed under a reducing diagenetic environment and the bottom red sediments, which have a high oxygen fugacity, are the result of the high geothermal temperature triggering the gas−liquid fluid cycle in the basin and the haematite generation in the bottom sediments. Additionally, Fig. 3 shows that there is no obvious peak at 435 nm for the DRS first derivative curves. This is because the Fe^{3+}/Fe^{2+} ratios of gray-black and gray–white sediments are less than 1, indicating that iron in the non-red sediments at the upper part of the borehole mainly exists in a low valence state and formed in a reducing diagenetic environment. Namely, trivalent iron oxides cannot exist stably, leading to no 435 nm peak. Meanwhile, the hematite in the underlying red sediment layer is long columnar, *i.e.*, goethite pseudocrystals, indicating that goethite may have been dehydrated and transformed into hematite.

Chen and Grapes (2007) proposed that the SE China red-bed sequence may be closely related to Mesozoic granite, acquiring their red colour on account of heat conduction from the intracrustal granitic magma layer beneath them. The paleo-Pacific (Kula) Plate subducting beneath SE China in Mesozoic lead to the crustal deformation as well as a large-scale crustal melting of fertile quartzo-feldspathic lithologies along the continental margins (Chen and Grapes, 2007). Furthermore, various types of structural basins occurred in different development stages of the widespread Mesozoic granite magma layer at the middle–upper crustal level. In the Late Triassic to Middle Jurassic, the fold basin occurring for the increase of crustal temperatures may be a result of Earth's thermal cycles (Tang and Li, 2016). In the Cretaceous–Paleogene, continental

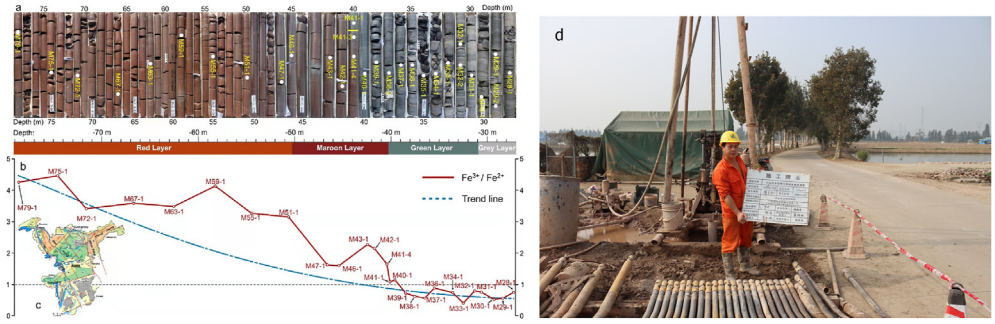

Fig. 2. a. Photographs of the borehole and sampling position showing stratigraphic columns with the relatively weakly weathered rock at a depth of approximately 27 m, and the end occurs at a depth of 79 m. At depths within 27–36.5 m, the rock is mainly grey dark lamellae mudstone interbedded with lamellae silty mudstone; from 36.5 to 40.15 m, cinerous hornfels is present, and below 40.15 m, maroon (40.15–50.1 m) and red (50.1–79 m) mudstone are present; b. calculated Fe^{3+}/Fe^{2+} ratios (from XRF and ferrous titration analyses) of the samples, which increase gradually (0.39–4.45) with depth. The ratios for the grey dark and cinerous sediments are <1, indicating that Fe mainly occurs in a low valence state in shallow-stratum non-red sediments, which formed in a reducing diagenetic environment. The ratios for the underlying red beds are >1 (maroon bed ratios of 1–3; red bed ratios >3), indicating that more Fe occurs in a high valence state at burial depth in red beds, which form in an oxidising diagenetic environment; c. borehole location, at which the borehole was drilled in red beds in SE China; d. drilling site.

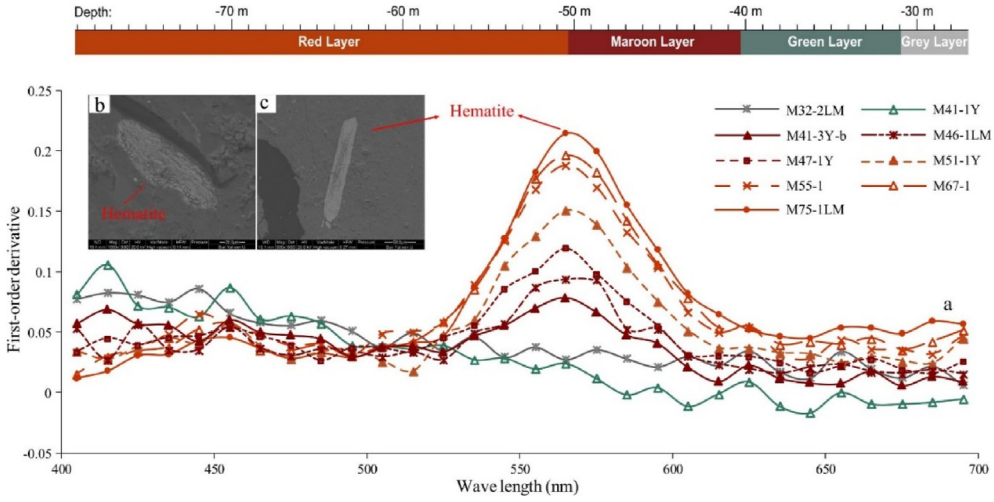

Fig. 3. a. DRS 1st derivative curves for the core sediment samples. The curves for the grey dark and cinerous sediments show no obvious ferric oxide peaks, and those for the underlying red beds show 565 nm haematite peaks with heights gradually increasing for deeper burial depths, without a 435 nm goethite peak but with 455 nm clay mineral peaks appearing; b. and c. haematite grains in the red sediment (M72-1) via SEM BSE imaging. The grains are anhedral and columnar, *i.e.*, in goethite pseudomorphs, implying that the haematite may have formed via goethite dehydration during sediment diagenesis.

red-bed basin developed as a result of extensional block faulting with the energy released by the crustal melting accumulated sufficiently. Due to the fault block basin deepend and their bottom sunk into the subjacent semiconsolidated granitic magma, temperatures within the basinal sediments rise, which may trigger goethite dehydration to haematite giving the sediment red colour when their temperatures reaching150 °C (Jiang et al., 2015). The formation of a complete red-bed system is the result of the high geothermal temperature triggering the gas−liquid fluid cycle in the basin and the haematite generation in the bottom sediments (Chen and Grapes, 2007).

3. Result and discussion

The idea of thermal fluctuation of the heat source from the interior of Earth (Tang and Li, 2016) may provide a solution to the climate–thermal paradox for the origin of continental red beds. Alternative warming and cooling have occurred many times throughout the history of Earth. In addition, active and quiescent periods of geological activity have alternatively occurred. We (specifically, C.T.) proposed that there exists a fundamental relationship between the thermal cycles and the episodic geological processes (Tang and Li, 2016). Possible causes of transferring heat out of the Earth range from magma oceans and plate tectonics to stagnant-lid convection. Global-scale rifting or ridge locking has acted as the major mechanism to trigger this thermal fluctuation, allowing transitions to occur between warming and cooling, with episodic tectonic activities. Van Kranendonk and Kirkland (2016) recognised that the periods of supercontinent assembly can be identified by relatively hot mantle, as documented by the rock record of mantle superplumes (or upwellings), komatiite, large igneous provinces, and accelerating crustal recycling. However, the periods of supercontinent dispersion can be identified by

relatively cool mantle as well as an increased proportion (but lower volume) of juvenile mantle magmatism. Actually, the alternating hot and cool mantle periods represent the underlying conditioned duality of the Earth system affected by the supercontinent cycles. Five cycles of supercontinent aggregation and dispersal can be identified (Van Kranendonk and Kirkland, 2016), which implies at least five thermal cycles.

In our opinion, the origin of continental red beds is a thermal abnormality rather than as a result of climate warming. If we are correct, it can be inferred that climate warming should immediately follow the continental red bed formation as a thermal effect, and this gives a reasonable explanation for why the seawater temperature was the highest at the western North Atlantic during the Turonian (Wilson et al., 2002) and the South Atlantic Oceans, in which warming had continued to the Campanian (Stoll and Schrag, 2000). The Turonian sea surface temperature (SST) was at least as warm as ~30 °C (conservative mean), or greatly warmer (~33 °C, or even higher than 36 °C), than that of the region today (Wilson et al., 2002). Earth's climate environment has fluctuated between greenhouse (warm) and icehouse (cold) modes during the Phanerozoic. One representative period of a typical greenhouse, with evidence of a large increase in CO_2 caused by frequent global igneous activities, is the Cretaceous–early Cenozoic era. Particularly, the mid-Cretaceous can be marked by a great warming crest, characterised by the global average surface temperature that was more than 14 °C higher than today (Tarduno et al., 1998), the absence of permanent ice covers (Frakes et al., 1992), and a sea level that was 100–200 m higher than today (Haq et al., 1987). Besides, the atmospheric carbon dioxide level is supposed to be 4 to 10 times higher than the preindustrial era. Geologic records also demonstrate that high-latitude temperatures between ca. 100–80 Ma in the middle Cretaceous had researched the warmest in Earth's history.

Oceanic anoxic events (OAEs) are the consequence of extremely hot or cold oceanic bottom waters caused by thermal fluctuations. Although as a global phenomenon, the term of OAEs has been proposed for more than 40 years ago (Schlanger and Jenkyns, 1976), it remains a concerned topic relevant to the significant points of the abundant organics buried in deep-sea sediments, the carbon cycling and its influence on the global climate. During the Cretaceous, as part of an OAE, black shales with 2–30% organic carbon were almost episodically deposited into oceanic and marginal basins (Erba, 2004). Besides, the deposition conditions have been widely investigated considering the significance of high marine productivity versus oceanic water stratification and stagnation. Altogether, cretaceous oceanic sediments have recorded eight intervals of OAEs (Erba, 2004). Between the OAEs, the unusual quiescences of global tectonic movements were caused by reduced thermal flux, resulting in oceanic bottom water temperatures lower than those necessary for red bed formation. The onset of widespread temperature increases under the oceanic bottom during the middle Ediacaran might be responsible for substantial changes in marine red bed (MRB) formation. Thus, MRBs following OAEs can be regarded as evidence for thermal episodes appearing during the long-term intervals of ocean crust thermal cycles. Further, their occurrence in the middle Ediacaran can restrict the timing of oceanic bottom thermal cycles.

If it is true that the red beds originated from the high diagenetic temperature, which is irrelevant to an arid paleoclimate, it is necessary to reconsider the factor controlling the global red bed distribution in different geological periods. After recoding their spatial distribution information, we found that the global red beds of different geological periods were closely associated with contemporaneous tectonic–magma belts, *e.g.*, the Paleozoic red beds are predominantly distributed along the Caledonian orogenic belt or the Variscan orogenic belt; the Meso-Cenozoic red beds are distributed along the circum-Pacific, the Tethys tecto-magma belts and the margins of the Meso-Cenozoic rifts (Fig. 4). These distributions suggest that red bed formation is relevant to tectonic movements under high

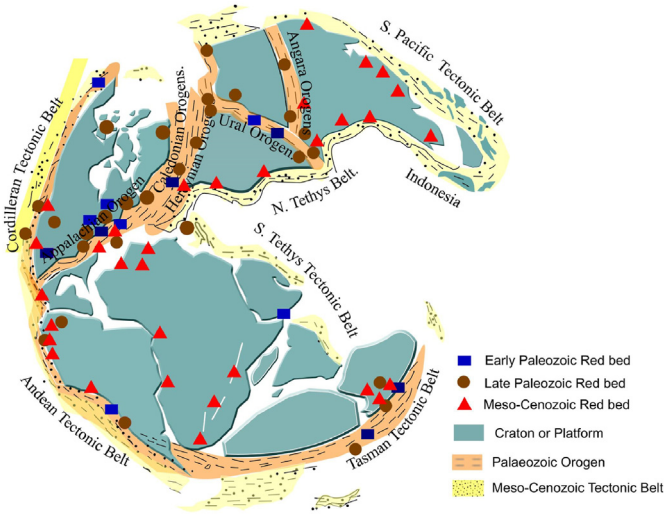

Fig. 4. Global red bed distribution in different geological periods, which is closely associated with contemporaneous tectonic–magma belts. The datum points were projected onto Pangea supercontinent (Seyfert and Sirkin, 1979), for the purple rectangles and brown dots from Seyfert and Sirkin (1979), for the red triangles from Seyfert and Sirkin (1979) and Chen and Grapes (2007). The Paleozoic red beds were predominantly distributed in the foredeep basins and intermountain basins along the Caledonian orogenic belt, *i.e.*, from Northern Europe and Greenland to northeast North America on the North America–Russia ancient continent or along the Varisian orogenic belt in the North America–Russia ancient continent and north Gondwanaland (Morris et al., 2010), in the Late Ordovician, in which thick continental red shale, sandstone and conglomerate were deposited in the depression between the fold uplift zone of the Appalachian orogenic belt and Laurentia (Torsvik, 1988); late Silurian red beds developed widely in several basins in the north–central United States; in addition, Ordovician and Silurian red beds developed in Australia in Gondwanaland (Petters, 1979). The Meso-Cenozoic red beds (Melinte and Jipa, 2005) were distributed along the circum-Pacific and the Tethys tectono-magma belts, which are closely related to the coeval granites, as well as the margins of the Meso-Cenozoic rifts, *e.g.*, the Triassic red beds were mainly distributed in North America, south–central Europe, east Australia, south Africa and India (Melchor, 2004), the Jurassic red beds were widely developed from Canada to central America (Jamison and Stearns, 1982), and the Cretaceous red beds were distributed in most of Gondwanaland, which began to separate (Tong et al., 2017). In the Cenozoic, red beds developed along the Tethys tectonic belt from Central Asia to southeastern China, in the piedmont depression of the European Alps, and along the margin of the Great Rift Valley in southeastern Africa and southern Australia (Singh et al., 2021).

geotemperatures but not to climatic factors. Therefore, red bed formation is a consequence of energy exchange between the sediment sphere and the lithosphere but not between the atmosphere and the sun.

A genetic association of large continental red bed accumulations with temporal (thermal cycle) and spatial (tectonic active zones) distribution provides support for the thermal genesis of red beds. Statistical analysis of the temporal and spatial distributions of Ediacaran and Phanerozoic MRBs shows that they are temporally related to the Earth's thermal cycles and spatially related to tectonically active zones. MRBs widely developed beyond the Cretaceous, occurring in sporadic intervals initially from the middle Ediacaran and throughout the Phanerozoic, and their first global distribution appeared in the middle Ediacaran (~580 million years ago) strata[18]. Both paleolatitude and geographical extent indicate that the Ediacaran and Phanerozoic MRBs were not localise, but worldwide (Fig. 4). In total, five global MRB intervals since the Phanerozoic have been documented, *i.e.*, Cambrian, Late Devonian, Early Triassic, Jurassic & Cretaceous episodes (Song et al., 2017). The Phanerozoic MRBs are typically composed of red carbonate and red mudstone, alternating with grey carbonate sometimes. Sedimentological, petrographic and mineralogical analyses of the Cretaceous MRBs imply that nanometre-scale haematite and goethite (mostly transformed into haematite during late diagenesis) are the main colouring agents of MRBs (25–27).

Millot (1970) claimed the relationship between the origin of red beds and tectonically active zones by emphasising the role of nonmarine environment & the abundant supply of little-altered detritus in orogenic belts. He pointed out that the clues to the geography of post-Hercynian red bed deposits of both Europe and North Africa could be well sought in the various Cenozoic molasse of the Alpine chain. Additionally, multi-stages of deformation along orogenic belts created a succession of molassic red bed deposits. Many desert red beds containing distinct border conglomerates deposited inside rift valleys (Van Houten, 1973), which can be considered a thermal channel to the interior of the Earth. The tectonic background which generally creats the geographic environment favouring accumulation of the common wedges of red beds and mottled sediments is the late to post-orogenic framework. Meckel (67) re-established one typical succession in the central Appalachians, in which the thick nonmarine wedges deposited at the close of three Paleozoic orogenies (Van Houten, 1973).

Continental red beds often occur alongside the margins of plateau-like uplifts, in which mechanical disintegration of rocks occurred. Irons could be transported to the surface by spring water in the form of bicarbonates. After discharge, the spring water would deposit ferrihydrite, the flakes of which were brought by river water or seasonal streams to the sedimentation areas. Then, they could deposit accompanied with the detrital material. During the diagenesis process, ferrihydrite spontaneously altered into haematite because of the absence of substantial quantities of organic matters (Chukhrov, 1973).

4. Conclusion

Our findings support a possible thermal origin of continental red beds. It can be inferred that the subsiding red-bed basins are heated from below rather than warmed from above. The continental red bed originates from the energy (thermal) exchange between the deep crustal heat source and the basin sediments, which is the consequence of endogenous thermal conduction of the Earth.

Before the appearance of terrestrial vegetation, the formation environment of continental red beds was particularly favourable and existed across vast territories because there were no abundance of terrestrial organic matters depositing in the continental sediments, mainly due to the very high temperature of the Earth. After the appearance of terrestrial vegetation, the amount of organic matters in continental sediments rised up, but only in tectonically active zones, such as in margins or basins, where the red beds were generating. This process was often local but still can be global. As the terrestrial vegetation flourished and due to the global-scale high temperature drop, the spatial distribution of the continental red beds altered into the areas of higher geothermal temperature with a surficial arid climate as a consequence. Therefore, before the appearance of vegetation, red bed might form in different latitudinal zones of the Earth. Thereafter, it became an indicator of a local thermal high temperature with a periodically dry, warm to hot climate (Chukhrov, 1973).

Our results add to the view that continental red bed *per se* is not a necessarily reliable indicators of climates. Furthermore, if we are correct, climate warming could immediately follow the continental red bed formation as a thermal effect. The continental red beds accompanied with evaporites possibly formed in response to a thermal high rather than an arid climate. Therefore, continental red bed should not be regarded as an indicator of any specific type of climate, and further evidence is needed to understand how the thermal energy promotes the conditions beneficial to haematite formation and preservation. However, the presence of haematite in continental red beds is an effective indicator of the Eh and pH of the interstitial environment regardless of climate (Walker, 1967). Although our finding cannot exclude the possibility that a low sedimentation rate in low-temperature environments may also play a role in the origin of red beds, the evidence that their formation was often constrained to short stratigraphic intervals (Walker, 1967; Song et al., 2017) requires an event-like triggering mechanism, and the quick conversion under high-temperature thermal anomalies seems more reasonable.

Data availability

The data underpinning this publication can be accessed from Brunel University London's data repository, Brunelfigshare here under a CCBY licence: https://doi.org/10.17633/rd.brunel.25952824.

CRediT authorship contribution statement

Lianting Jiang: Data curation, Formal analysis, Investigation, Writing – original draft, Funding acquisition. **Chun'an Tang:** Conceptualization, Methodology, Supervision, Writing – review & editing, Funding acquisition. **Bin Gong:** Investigation, Methodology, Supervision, Writing – review & editing. **Zhen Chen:** Investigation, Validation, Writing – review & editing. **Tiantian Chen:** Formal analysis, Visualization, Writing – review & editing. **Zhanjie Qin:** Formal analysis, Visualization, Writing – review & editing. **Guoneng Chen:** Resources, Validation, Writing – review & editing, Funding acquisition.

Declaration of competing interest

The authors declare that they have no known competing financial interests or personal relationships that could have appeared to influence the work reported in this paper.

Acknowledgments

This work was funded by the Original Exploration Project of the National Natural Science Foundation of China, China (Grant No. 42050201), the general project of the State Key Laboratory of Geological Processes and Mineral Resources (China University of Geosciences (Wuhan)), China (Grant No. GPMR202002), the special fund for Special Project of Geological Hazard Control, Guangdong Province, China (Grant No. 2017201), the multi-element three-dimensional urban geological survey project of Zhongshan City, China (Grant No. 442000-201903-2019001-0011 (ZZ21909738)), and the Science and Technology Projects of Guangzhou, China (Grant No. 202201010638).

References

Bowers, H.E., Shawe, D.R., 1961. Heavy Minerals as Guides to Uranium-Vanadium Are Deposits in the Split Rock District, Colorado. United States Government Printing Office, Washington.

Cai, Y.F., Hu, X.X., Li, X., Pan, Y.G., 2012. Origin of the red colour in a red limestone from the Vispi Quarry section (Central Italy): a high-resolution transmission electron microscopy analysis. Cretac. Res. 38, 97–102.

Chen, G.N., Grapes, R., 2007. Granite Genesis: In-Situ Melting and Crustal Evolution. Springer, Dordrecht, pp. 187–228.

Chukhrov, F.V., 1973. On mineralogical and geochemical criteria in the genesis of red beds. Chem. Geol. 12, 67–75.

Erba, E., 2004. Calcareous nannofossils and Mesozoic oceanic events. Mar. Micropaleontol. 52, 85–106.

Frakes, L.A., Francis, J.E., Syktus, J.I., 1992. Climate Modes of the Phanerozoic. Cambridge University Press, Cambridge.

Haq, B.U., Hardenbol, J., Vail, P.R., 1987. Chronology of fluctuating sea levels since the Triassic. Science 235, 1156–1167.

Jamison, W.R., Stearns, D.W., 1982. Tectonic deformation of wingate sandstone, Colorado National Monument. AAPG (Am. Assoc. Pet. Geol.) Bull. 66, 2584–2608.

Jiang, L.T., Chen, G.N., Grapes, R., Peng, Z.L., 2015. Thermal origin of continental red beds in SE China: an experiment study. J. Asian Earth Sci. 101, 14–19.

Li, X., Chen, S., Cao, K., Chen, Y., Xu, B., Ji, Y., 2009. Paleosols of the mid-cretaceous: a report from zhejiang and fujian, SE China. Earth Sci. Front. 16, 63–70.

Melchor, R.N., 2004. Trace fossil distribution in lacustrine deltas: examples from the Triassic rift lakes of the Ischigualasto-Villa Unión basin, Argentina. In: Mcllroy, D. (Ed.), The Application of Ichnology to Palaeoenvironmental and Stratigraphic Analysis. Geological Society Special Publication, London.

Melinte, M.C., Jipa, D., 2005. Campanian-Maastrichtian marine red beds in Romania: biostratigraphic and genetic significance. Cretac. Res. 26, 49–56.

Millot, G., 1970. Geology of Clays. Springer, Berlin.

Morris, T.H., Ritter, S.M., Laycock, D.P., 2010. Geology Unfolded: an Illustrated Guide to the Geology of Utah's National Parks. Young University Press, Brigham.

Petters, S.W., 1979. West African cratonic stratigraphic sequences. Geology 7, 528–531.

Picard, M.D., 1971. Petrographic criteria for recognition of lacustrine and fluvial sandstone. In: Utah Geological and Mineralogical Survey. University of Utah, Utah.

Schlanger, S.O., Jenkyns, H.C., 1976. Cretaceous oceanic anoxic events: causes and consequences. Geol. Mijnbouw 55, 179–184.

Schmalz, R.F., 1968. Formation of red beds in modern and ancient deserts: discussion. GSA Bulletin 79, 277–280.

Seyfert, C.K., Sirkin, L.A., 1979. Earth History and Plate Tectonics. Harper & Row, New York.

Singh, S., Awasthi, A.K., Khanna, Y., Kumari, A., Singh, B., Kumar, A., Popli, C., 2021. Sediment colour as recorder of climate and tectonics: Cenozoic continental red beds of the Himalayan foreland basin in NW India. Catena 203, 105298.

Song, H., Jiang, G., Poulton, S.W., Wignall, P.B., Tong, J., Song, H., An, Z., Chu, D., Tian, L., She, Z., Wang, C., 2017. The onset of widespread marine red beds and the evolution of ferruginous oceans. Nat. Commun. 8, 399.

Stoll, H.M., Schrag, D.P., 2000. High-resolution stable records from the Upper Cretaceous rocks of Italy and Spain: glacial episodes in a greenhouse planet? GSA Bulletin 112, 308–319.

Tang, C.A., Li, S.Z., 2016. The Earth evolution as a thermal system. Geol. J. 51, 652–668.

Tarduno, J.A., Brinkman, D.B., Renne, P.R., Cottrell, R.D., Scher, H., Castillo, P., 1998. Evidence for extreme climatic warmth from Late Cretaceous Arctic vertebrates. Science 282, 2241–2243.

Tong, Y., Yang, Z., Pei, J., Wang, H., Xu, Y., Pu, Z., 2017. Paleomagnetism of the Upper Cretaceous red-beds from the eastern edge of the Lhasa Terrane: new constraints on the onset of the India-Eurasia collision and latitudinal crustal shortening in southern Eurasia. Gondwana Res. 48, 86–100.

Torsvik, T.H., Sturt, B.A., Ramsay, D.M., Bering, D., Fluge, P.R., 1988. Palaeomagnetism, magnetic fabrics and the structural style of the hornelen old red sandstone, western Norway. J. Geol. Soc. 145, 413–430.

Turner, P., 1980. Continental Red Beds. Elsevier Scientific Publishing Company, Amsterdam.

Van Houten, F.B., 1973. Origin of red beds: a review-1961-1972. Annu. Rev. Earth Planet Sci. 1, 39–61.

Van Kranendonk, M.J., Kirkland, C.L., 2016. Conditioned duality of the earth system: geochemical tracing of the supercontinent cycle through earth history. Earth Sci. Rev. 160, 171–187.

Walker, T.R., 1967. Formation of red beds in modem and ancient deserts. GSA Bulletin 78, 353–368.

Wang, X.L., Wang, Q., Jiang, X.S., Cheng, X., Zhang, J.L., Zhao, Z.K., Jiang, Y.E., 2012. Dinosaur egg faunas of the Upper Cretaceous terrestrial red beds of China and their stratigraphical significance. J. Stratigr. 36, 400–416.

Weibel, R., Grobety, B., 1999. Effects of burial on the clay assemblages in the triassic Skagerrak Formation, Denmark. Clay Miner. 34, 619–635.

Wilson, P.A., Norris, R.D., Cooper, M.J., 2002. Testing the Cretaceous greenhouse hypothesis using glassy foraminiferal calcite from the core of the Turonian tropics on Demerara Rise. Geology 30, 607–610.

Xue, G.Y., Lou, W.P., Zhang, W.X., Wu, C.H., He, F.P., 2005. Analysis on ancient climate characteristics in SE China in the Early Cretaceous period based on the Xinchang petrified wood. Journal of Nanjing Institute of Meteorology 28, 666–671.